Flexible, Polymer-Supported, Si Wire Array Photoelectrodes

By *Joshua M. Spurgeon, Shannon W. Boettcher, Michael D. Kelzenberg, Bruce S. Brunschwig, Harry A. Atwater,** and *Nathan S. Lewis**

In contrast to brittle, ultrahigh purity silicon wafers used to produce conventional crystalline Si-based solar cells, device physics modeling shows that silicon wires with radial junctions can achieve high energy-conversion efficiencies using material that has a low ratio of minority-carrier collection length to optical absorption depth.[1] Si wire studies[2,3] and wire-based solar cell reports[4–10] suggest that this is an attractive approach to photovoltaic design. We have recently reported the growth and transfer of arrays of highly oriented crystalline Si wires into flexible, optically transparent, polydimethylsiloxane (PDMS) films,[11,12] and the reuse of the Si growth substrate to fabricate multiple subsequent arrays.[13] Herein we demonstrate that flexible, freestanding, polymer-supported Si wire array electrodes in liquid-junction photoelectrochemical cells yield current–potential behavior similar to that of the Si wires attached to the growth substrate. The quantum yield of the polymer-supported wire array photoelectrodes as a function of wavelength and angle of incidence indicates that the devices produce more photocurrent than expected based solely on the geometric packing fraction of the Si wires. These systems offer the potential for attaining high solar energy-conversion efficiencies using modest diffusion length, readily grown, crystalline Si absorbers in a flexible, processable form factor.

Figure 1a and **1b** show representative scanning electron microscopy (SEM) images of substrate-attached and peeled, polymer-supported Si wire arrays, respectively. The wires were grown by the vapor-liquid-solid (VLS) method[14] from Cu catalyst deposited in lithographically defined holes in a Si oxide buffer layer on the surface of a (111)-oriented Si growth substrate.[11] Cu was chosen instead of the more commonly used Au as the growth catalyst, due to the higher abundance of Cu in the Earth's crust as well as the less deleterious effect of Cu as an impurity in p-Si based solar cells.[15] Minority-carrier collection lengths >10 μm have been measured on individual Si microwires grown by this method.[16] Thus, the ~1.5 μm radius of the microwires should enable efficient radial minority-carrier collection while their 100 μm length (Figure 1a) is comparable to the planar thickness required for efficient absorption of photons with energies greater than the 1.1 eV indirect band gap of Si. The wire arrays were infiltrated with PDMS and peeled off of the growth substrate, yielding a flexible, processable material consisting of an ordered array of crystalline Si wires with their bases embedded in, but most of their length projecting out from, the PDMS film (Figure 1b and 1c). An ohmic contact to the wires was made by evaporating ~300 nm of Au onto the back side of the PDMS film. The polymer/wire composite films were subsequently attached to a Ti foil to facilitate their use as photoelectrodes. Replacement of this foil with a bendable current collector would yield a fully flexible device. Current–voltage measurements using a microprobe station on the polymer-supported wire arrays showed that essentially all of the wires were contacted (see Supporting Information). The photoelectrochemical energy-conversion properties of these polymer-supported wire arrays were compared to the performance of a photoactive, planar crystalline Si bulk electrode as well as to the performance of an array of nominally identical VLS-grown Si wires that were physically attached to their photoinactive, p^+-Si growth substrate.

A photoelectrochemical cell with a methyl viologen (MV^{2+}/MV^+) redox species (Figure 1d) was used to produce a conformal radial junction to each wire in the array. The formation of a semiconductor/liquid junction obviated the complexity of producing high-quality radial solid-state junctions, transparent conductors, and metallic grid emitter contacts to evaluate the energy-conversion performance of the wire arrays. Although Si wire array photoelectrochemical cells reported to date have demonstrated low efficiencies (ca. 0.1%),[4,5] we have recently shown that significantly improved performance, as measured in an aqueous methyl viologen redox system, can be obtained with substrate-attached arrays by controlled p-type doping through the in-situ addition of BCl_3 during the growth of Cu-catalyzed p-Si wires.[17] The solution permeated the full length of the wire array to form a highly rectifying, conformal contact with p-Si.[18,19] Under illumination conditions that produced short-circuit photocurrent densities (J_{sc}) of 25 mA cm^{-2} on planar, crystalline Si(111) samples, this system yielded open-circuit voltages (V_{oc}) > 550 mV, close to the bulk diffusion/recombination limit. The MV^+ radical cation is highly absorbing across much of the visible (350–750 nm) spectrum,[20] which gives the electrolyte an intense, violet color. To minimize confounding effects due to solution absorbance, 808 nm laser light was used to excite the Si photoelectrodes in all of the comparisons reported herein. A calibrated photodiode was placed in the solution at the height of the wire array electrode to monitor the in situ illumination intensity.

[*] Dr. J. M. Spurgeon, Dr. S. W. Boettcher, Dr. B. S. Brunschwig, Prof. N. S. Lewis
California Institute of Technology
Division of Chemistry and Chemical Engineering
1200 E. California Blvd. m/c 127-72
Pasadena, CA 91125 (USA)
E-mail: nslewis@caltech.edu
M. D. Kelzenberg, Prof. H. A. Atwater
California Institute of Technology
Division of Engineering and Applied Science
1200 E. California Blvd. m/c 128-95
Pasadena, CA 91125 (USA)
E-mail: haa@caltech.edu

DOI: 10.1002/adma.201000602

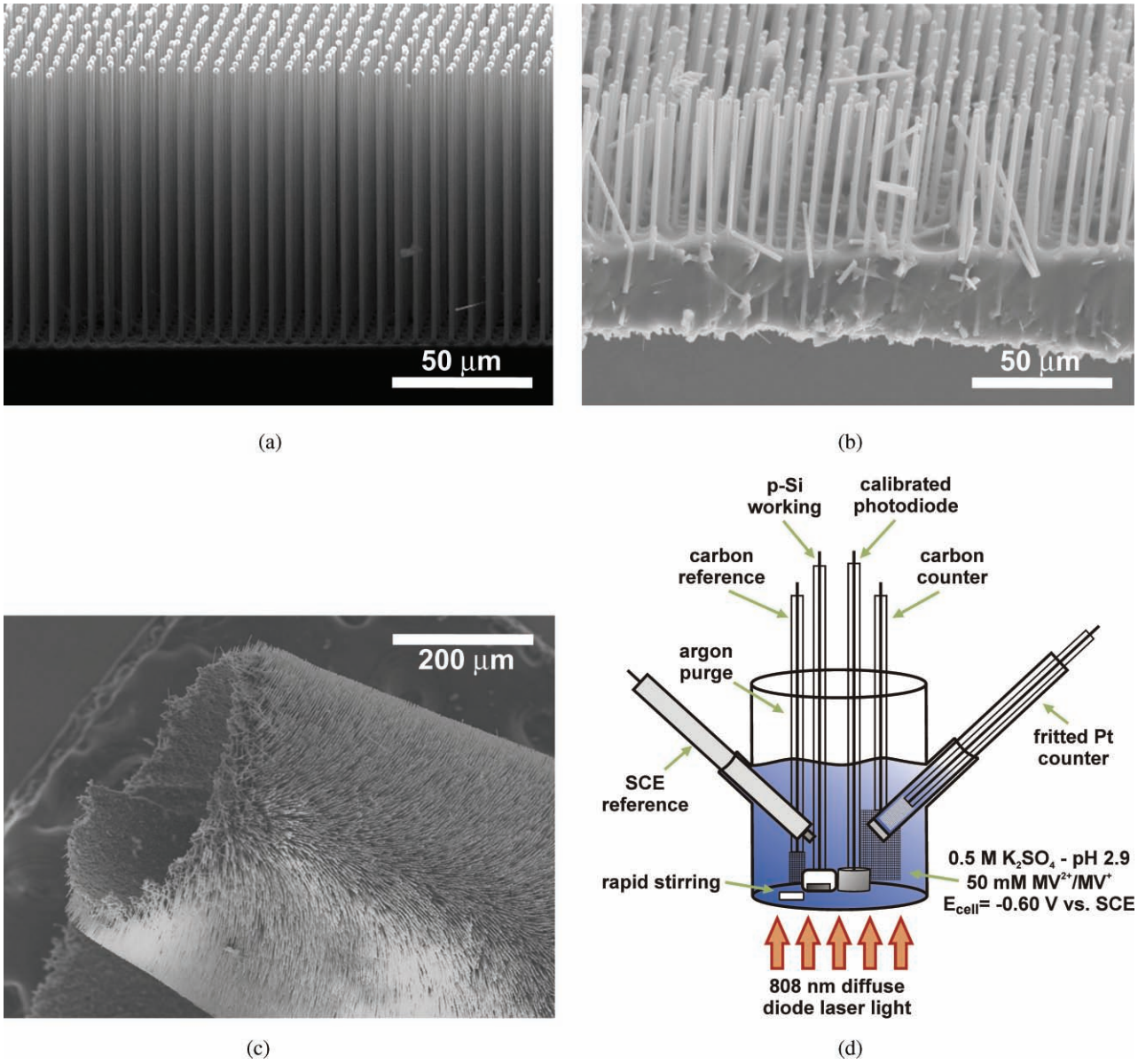

Figure 1. Wire arrays and photoelectrochemical cell setup. Cross-sectional SEM images of (a) a substrate-attached wire array (before Cu etch) and (b) a peeled, polymer-supported wire array. The PDMS layer in (b) was deliberately made thicker than was typically used to make photoelectrodes, to facilitate SEM imaging of the structure. (c) SEM image of a peeled, polymer-supported wire array demonstrating the flexibility of these films. (d) Diagram of the cell setup that was used for the photoelectrochemical measurements (see Experimental).

The current density vs. potential (*J*–*E*) behavior of substrate-attached wire arrays and of polymer-supported wire arrays was measured and compared to that of a planar p-Si wafer. The *J*–*E* data at various light intensities are displayed on a common graph (**Figure 2**) by presenting the data in terms of the measured external quantum yield (Φ_{ext}, electrons collected per incident photon), which is directly proportional to the observed photocurrent density (see Supporting Information). As shown in Figure 2a, at light intensitie$\sigma \leq 40$ mW cm^{-2}, the planar p-Si photoelectrode exhibited $\Phi_{ext} \sim 0.7$, in accord with the value expected for specularly reflective, high-quality bulk Si samples (~30% reflectance).[21] The decline in the short-circuit external quantum yield ($\Phi_{ext,sc}$) at higher light intensities resulted from mass-transport effects in the solution, at the concentration of redox species used in this test electrolyte. The increase in open-circuit voltage with illumination intensity occurred because of the logarithmic dependence of V_{oc} on the photocurrent.

Figure 2b and 2c depict the Φ_{ext} vs. *E* behavior of substrate-attached and peeled, polymer-supported, Si wire array photoelectrodes, respectively. The photoelectrochemical response observed from the substrate-attached wire arrays arose primarily from the Si wires, because as established previously, the presence of the thermal oxide, combined with the use of degenerately doped p-Si substrates, minimized the photoelectrochemical response

from the substrate.[17] The Φ_{ext} vs. E behavior of the polymer-supported wire arrays was very similar to that of the wire array on the growth substrate (Figure 2d). The most noticeable difference was in the fill factor, which improved after casting the PDMS into the Si wires (even if the array was not peeled from the substrate), consistent with the presence of shunts through the base of the substrate-attached, PDMS-free wire arrays. The fill factor of photoelectrodes made from substrate-attached wire arrays that were not supported in PDMS (Figure 2b) improved significantly when a surface etch was performed immediately prior to measurement of the Φ_{ext} vs. E behavior (not shown),[17] suggesting that a Cu-rich surface layer might still be present on the wires despite the use of a Cu etch prior to electrode fabrication. However, this etch caused irreversible damage to the polymer-supported electrodes (see Supporting Information), precluding a direct comparison of the array performance under these more optimal conditions.

The $\Phi_{ext,sc}$ values observed for polymer-supported wire array photoelectrodes were slightly lower than those observed for substrate-attached wire arrays without PDMS (**Table 1**, Figure 2d). This difference is expected because PDMS covered the bottom 10–20 μm of the Si wires, preventing those regions from directly exchanging current with the electrolyte. The observed $\Phi_{ext,sc}$ = 0.2–0.3 for the wire arrays is significant, especially considering that the packing fraction (percentage of the cross-sectional device area occupied by wires) of the array was only ~4%. Without enhanced photon capture, a 4% packing fraction would result in a $\Phi_{ext,sc}$ of ≤0.04 at normal incidence.

The V_{oc} values measured for wire array photoelectrodes, although ~150 mV lower than those of the planar electrode, are higher than those previously measured on Si nanowire arrays.[4–9] The decrease in V_{oc} is attributable to increased dark current due to the increased junction area of the wire array relative to the planar electrode, and to the increased effects of surface recombination.[22] Decreasing the wire size from the ~1.5 μm radius investigated herein while maintaining a similar packing fraction would thus be expected to result in a lower V_{oc} without a concomitant increase in J_{sc}, in accord with the lower photovoltages observed for photoelectrodes formed using Si nanowires.[6–9]

Assessing the intrinsic photoelectrochemical behavior of the wire array electrodes requires correction for the concentration

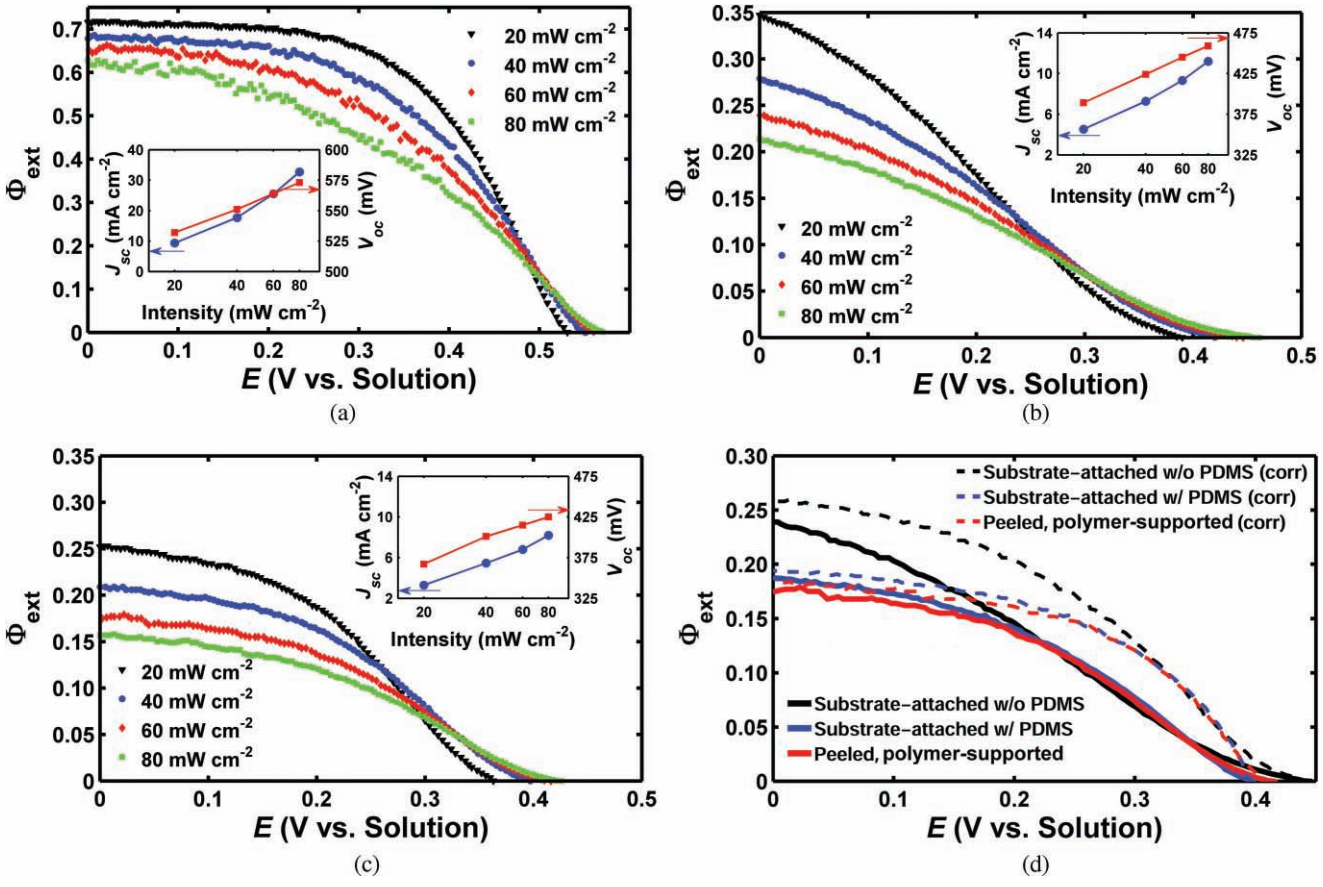

Figure 2. Effect of intensity and electrode type on cell performance. Plots of external quantum yield (Φ_{ext}) vs. potential (E) for different illumination intensities using (a) a planar, (b) a substrate-attached wire array without PDMS, and (c) a peeled, polymer-supported wire array photoelectrode. Insets show semilogarithmic (lin-log) plots of J_{sc} and V_{oc} vs. intensity. (d) Plot comparing the performance of a substrate-attached wire array without PDMS, a substrate-attached wire array with PDMS cast on it, and a peeled, polymer-supported wire array electrode under 60 mW cm^{-2} illumination. Dashed lines are the photoelectrode behavior corrected for concentration overpotential and solution resistance losses. All three electrodes in (d) came from the same Si wire array sample.

Table 1. Wire array photoelectrochemical cell performance data.[a]

	Substrate-attached			
Intensity (mW cm^{-2})	20	40	60	80
$\Phi_{ext,sc}$	0.36 ± 0.06	0.29 ± 0.05	0.25 ± 0.05	0.22 ± 0.04
J_{sc} (mA cm^{-2})	4.6 ± 0.7	7.4 ± 1.3	9.8 ± 1.8	11.6 ± 2.1
V_{oc} (mV)	356 ± 21	398 ± 16	422 ± 16	437 ± 17
FF	0.26 ± 0.03	0.27 ± 0.02	0.27 ± 0.03	0.28 ± 0.03
η_{808} (%)[b]	2.2 ± 0.6	2.0 ± 0.6	1.9 ± 0.5	1.8 ± 0.5
$\eta_{808,corr}$ (%)[c]	3.1 ± 0.8	3.0 ± 0.8	2.8 ± 0.8	2.7 ± 0.8
	Peeled, polymer-supported			
Intensity (mW cm^{-2})	20	40	60	80
$\Phi_{ext,sc}$	0.27 ± 0.04	0.23 ± 0.04	0.20 ± 0.03	0.18 ± 0.03
J_{sc} (mA cm$^{-}{}_{2}$)	3.5 ± 0.5	6.0 ± 0.9	7.9 ± 1.3	9.6 ± 1.6
V_{oc} (mV)	339 ± 29	373 ± 29	390 ± 30	402 ± 31
FF	0.36 ± 0.05	0.36 ± 0.04	0.35 ± 0.05	0.35 ± 0.04
η_{808} (%)[b]	2.1 ± 0.3	2.0 ± 0.3	1.8 ± 0.2	1.6 ± 0.2
$\eta_{808,corr}$ (%)[c]	2.8 ± 0.4	2.8 ± 0.4	2.6 ± 0.4	2.4 ± 0.4

[a] Averages and standard errors were calculated using 10 different samples of both substrate-attached and peeled, polymer-supported wire arrays. [b,c] This efficiency is for monochromatic 808 nm illumination, [b] uncorrected and [c] corrected for concentration overpotential and uncompensated resistance losses.

overpotential and uncompensated resistance losses that arise from the use of the unoptimized test electrolyte (see Supporting Information).[23] The corrected Φ_{ext} vs. E behavior (Figure 2d, dashed lines) reveals the performance of the photoelectrodes that would be obtained in a thin-layer cell with minimal concentration overpotential and series resistance losses. The corrected efficiency values for each type of wire array photoelectrode are summarized in Table 1.

The spectral response properties of the photoelectrodes were evaluated as a function of the angle of incidence (**Figure 3**).[24] The $\Phi_{ext,sc}$ values observed at 808 nm were in good agreement with those measured at low light intensity using the 808 nm monochromatic diode laser. As observed previously, the quantum yield of the substrate-attached Si wire array photoelectrode was highly dependent on the angle of incidence.[17,24] At angles significantly off normal, the optical path length through the substrate-attached wires increased and less light passed completely in the regions between wires. Thus, significantly more light was absorbed and $\Phi_{ext,sc} > 0.6$ (Figure 3a). The spectral response of peeled, polymer-supported wire array electrodes also showed increased $\Phi_{ext,sc}$ at higher angles, with a maximum of $\Phi_{ext,sc} \sim 0.45$ (Figure 3b). The reduced dependence of $\Phi_{ext,sc}$ on the incidence angle for the peeled, polymer-supported wire arrays can be attributed to greater disorder in the array that led to enhanced light scattering (see Supporting Information).

The behavior of the peeled, polymer-supported Si wire film relative to the unpeeled, substrate-attached wire array electrode demonstrates that Si wires can be transferred into inexpensive, flexible films without sacrificing their solar energy-conversion performance. The single-wavelength Φ_{ext} and V_{oc} values reported herein are large compared to those reported for previous Si nanowire array solar cells, and the spectral response data showed high quantum yields across the entire visible spectrum. The peeled wire/polymer composite photoelectrodes had $\Phi_{ext,sc}$ values that ranged from 0.28 (approximately 7 times the packing fraction, ~4%) at normal incidence to 0.45 at high angles of incidence (~50°). By increasing the packing fraction and exploring designs that lengthen the path of light through the wires, external quantum yields approaching that of planar bulk Si should be attainable for the peeled wire array photoelectrodes.[24] With effective light-trapping, improving the J_{sc} to 35 mA cm^{-2} indicates that energy-conversion efficiencies > 5% are possible under AM 1.5 illumination even without improving the other characteristics of these polymer-supported wire array photoelectrodes.[25] The overpotential-corrected data demonstrate that still higher performance would be obtainable through the use of optimized liquid-junction or solid-state cell configurations, with efficiencies > 10% possible with additional modest improvements to the V_{oc} and fill factor. The results indicate that a flexible, Si wire array solar energy-conversion device with a competitive efficiency is possible based on wire array architectures that do not contain a supporting crystalline Si wafer nor utilize brittle, ultrahigh purity crystalline Si.

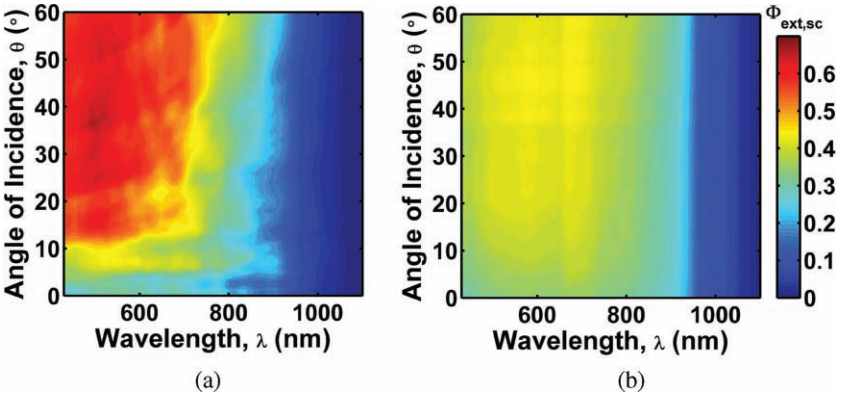

Figure 3. Si wire array spectral response. 2-dimensional color maps depicting the short-circuit quantum yield ($\Phi_{ext,sc}$) at low light intensity vs. wavelength and angle of incidence for (a) a substrate-attached wire array without PDMS and (b) a peeled, polymer-supported wire array, both in contact with an aqueous methyl viologen$^{2+/+}$ solution.

Experimental Section

Wire Array Electrode Fabrication: The Si wire array growth process has been described in detail elsewhere.[11] Wires were grown from Cu catalyst and doped p-type as previously published,[17] yielding wires 90 ± 15 μm long and ~1.5–1.7 μm in diameter, in a square arrangement of 7 μm pitch. Following growth at 1000 °C, the reactor tube was purged with N_2(g) and cooled over the course of ~30 min to ~750 °C before sample removal. A wire doping concentration of 10^{17} cm^{-3} was determined by a series of lithographically defined 4-point probe measurements on individual wires.[16]

Prior to electrode fabrication, each Si sample was etched for 10 s in 10% aq. HF, 10 min in 6: 1: 1 H_2O: 30% H_2O_2: concentrated HCl (v/v) at 70 °C (RCA2 clean), 10 s in 10% aq. HF, and 2 min in 20% aq. KOH. Samples were thoroughly rinsed in 18 MΩ-cm H_2O and dried with N_2(g) between each

step. This process removed the Cu catalyst tip and the surface layer of the wires, but left the thermal oxide on the substrate intact.

Wire arrays were infiltrated with polymer and stripped from the underlying wafer using a procedure that closely followed published methods.[12] 4.4 g of hexamethylcyclotrisiloxane (98%, Alfa Aesar) was dissolved in ~5 mL methylene chloride, then mixed with 1.1 g of Sylgard 184 polydimethylsiloxane (Dow Corning, 1.0 g PDMS base, 0.1 g PDMS curing agent). This mixture was spin-coated onto the wire arrays at 1000 rpm for 1 min, then heated at 150 °C for 30 min. This procedure produced a 10–20 μm thick layer of PDMS at the bases of the Si wires. Polymer-supported wire arrays were mechanically removed from the underlying Si substrate using a razor blade.

Planar photoelectrodes were made from 1–2 Ω-cm resistivity p-Si(111) wafers. Ohmic back contacts were made to the substrate-attached wire array and to the planar electrodes by rubbing a Ga/In eutectic mixture onto the back side of the wafer. To make back contacts to polymer-supported films, the samples were taped to a glass slide and ~300 nm of Au was evaporated onto the film. Polymer/wire films were affixed to Ti foil using conductive silver paint to facilitate the use of the films as photoelectrodes.

Immediately prior to use in the photoelectrochemical cell, polymer-supported electrodes were subjected to an oxygen plasma to remove any residual PDMS on the exposed Si wires and to convert the PDMS surface from hydrophobic to hydrophilic so that the aqueous liquid electrolyte could effectively penetrate the array. The plasma generator (March PX-500) was run for 180 s at 600 W with 330 mTorr O_2. Before photoelectrochemical measurements, each electrode was etched in 10% aq. HF for 10 s to remove the surface oxide.

Photoelectrochemical Cell: A flat-bottomed glass cell was filled with 50 mL of aqueous 0.05 M methyl viologen dichloride (MV^{2+}, Aldrich, 98%), 0.5 M K_2SO_4, buffered at pH = 2.9 using 0.1 M potassium hydrogen phthalate and sulfuric acid, and was continually purged with H_2O-saturated Ar. The cell contained a standard calomel reference electrode (SCE), a Pt mesh counter electrode separated from the main compartment by a glass frit, a large carbon cloth electrode, a small carbon cloth electrode, a Si working electrode (wire array or planar), and a calibrated Si photodiode (Thorlabs) positioned at the height of the working electrode (Figure 1d). A stir bar next to the Si electrode minimized mass-transport limitations.

Prior to measurement, the solution was electrolyzed to –0.60 V vs. SCE using the large carbon cloth as a working electrode, the Pt mesh as a counter electrode, and the SCE as a reference electrode. This process produced ~3 mM MV^+ and turned the solution dark violet ($E^{o'}(MV^{2+/+})$ = –0.67 V vs. SCE). The solution potential was adjusted periodically to maintain a value of –0.60 V vs. SCE. Current-potential data were obtained using the Si as the working electrode, the large carbon cloth as the counter electrode, and the small carbon cloth (poised at the solution potential) as the reference. A 1 W, 808-nm diode laser (Thorlabs L808P1WJ) provided an illumination source at a wavelength that minimized the solution absorbance. The power output of the laser was adjustable, and the photodiode was used to determine the light intensity on the Si working electrode. A Princeton Applied Research Model 273 potentiostat was used to collect the current-potential data.

Spectral Response: The apparatus and procedure used for spectral response measurements has been described in detail elsewhere.[24] The same aqueous methyl viologen electrolyte was used, with stirring, as for the Φ_{ext} vs. E measurements. Absolute V_{oc} values were not necessary, and hence optically transparent solutions were used ($[MV^{2+}]/[MV^+] >> 1$), allowing measurements across the full visible region of the spectrum.

Supporting Information

Supporting Information is available online from Wiley InterScience or from the author.

Acknowledgements

This work was financially supported by BP plc and by the Department of Energy, Office of Basic Energy Sciences, DE-FG02-07ER46405. BSB acknowledges support from the NSF Center for Chemical Innovation Grant No. 0802907 (Powering the Planet). We acknowledge use of facilities supported by the Caltech Center for Science and Engineering of Materials, an NSF MRSEC, and the Caltech Center for Sustainable Energy Research.

Received: February 16, 2010
Published online: June 29, 2010

[1] B. M. Kayes, H. A. Atwater, N. S. Lewis, *J. Appl. Phys.* **2005**, *97*.
[2] V. Schmidt, J. V. Wittemann, U. Gosele, *Chem. Rev.* **2010**, *110*, 361.
[3] L. J. Lauhon, M. S. Gudiksen, D. Wang, C. M. Lieber, *Nature* **2002**, *420*, 57.
[4] J. R. Maiolo, B. M. Kayes, M. A. Filler, M. C. Putnam, M. D. Kelzenberg, H. A. Atwater, N. S. Lewis, *J. Am. Chem. Soc.* **2007**, *129*, 12346.
[5] A. P. Goodey, S. M. Eichfeld, K. K. Lew, J. M. Redwing, T. E. Mallouk, *J. Am. Chem. Soc.* **2007**, *129*, 12344.
[6] B. Z. Tian, X. L. Zheng, T. J. Kempa, Y. Fang, N. F. Yu, G. H. Yu, J. L. Huang, C. M. Lieber, *Nature* **2007**, *449*, 885.
[7] L. Tsakalakos, J. Balch, J. Fronheiser, B. A. Korevaar, O. Sulima, J. Rand, *Appl. Phys. Lett.* **2007**, *91*.
[8] E. C. Garnett, P. D. Yang, *J. Am. Chem. Soc.* **2008**, *130*, 9224.
[9] T. Stelzner, M. Pietsch, G. Andra, F. Falk, E. Ose, S. Christiansen, *Nanotechnology* **2008**, *19*.
[10] Z. Y. Fan, H. Razavi, J. W. Do, A. Moriwaki, O. Ergen, Y. L. Chueh, P. W. Leu, J. C. Ho, T. Takahashi, L. A. Reichertz, S. Neale, K. Yu, M. Wu, J. W. Ager, A. Javey, *Nat. Mater.* **2009**, *8*, 648.
[11] B. M. Kayes, M. A. Filler, M. C. Putnam, M. D. Kelzenberg, N. S. Lewis, H. A. Atwater, *Appl. Phys. Lett.* **2007**, *91*.
[12] K. E. Plass, M. A. Filler, J. M. Spurgeon, B. M. Kayes, S. Maldonado, B. S. Brunschwig, H. A. Atwater, N. S. Lewis, *Adv. Mater.* **2009**, *21*, 325.
[13] J. M. Spurgeon, K. E. Plass, B. M. Kayes, B. S. Brunschwig, H. A. Atwater, N. S. Lewis, *Appl. Phys. Lett.* **2008**, *93*, 032112.
[14] R. S. Wagner, W. C. Ellis, *Appl. Phys. Lett.* **1964**, *4*, 89.
[15] J. R. Davis, A. Rohatgi, R. H. Hopkins, P. D. Blais, P. Raichoudhury, J. R. McCormick, H. C. Mollenkopf, *IEEE Trans. Electron Devices* **1980**, *27*, 677.
[16] M. C. Putnam, D. B. Turner-Evans, M. D. Kelzenberg, S. W. Boettcher, N. S. Lewis, H. A. Atwater, *Appl. Phys. Lett.* **2009**, *95*.
[17] S. W. Boettcher, J. M. Spurgeon, M. C. Putnam, E. L. Warren, D. B. Turner-Evans, M. D. Kelzenberg, J. R. Maiolo, H. A. Atwater, N. S. Lewis, *Science* **2010**, *327*, 185.
[18] D. C. Bookbinder, N. S. Lewis, M. G. Bradley, A. B. Bocarsly, M. S. Wrighton, *J. Am. Chem. Soc.* **1979**, *101*, 7721.
[19] E. S. Kooij, R. W. Despo, F. P. J. Mulders, J. J. Kelly, *J. Electroanal. Chem.* **1996**, *406*, 139.
[20] J. F. Stargardt, F. M. Hawkridge, *Anal. Chim. Acta* **1983**, *146*, 1.
[21] H. R. Philipp, E. A. Taft, *Phys. Rev.* **1960**, *120*, 37.
[22] J. M. Spurgeon, H. A. Atwater, N. S. Lewis, *J. Phys. Chem. C* **2008**, *112*, 6186.
[23] A. J. Bard, L. R. Faulkner, *Electrochemical Methods: Fundamentals and Applications*, John Wiley & Sons, New York **2001**.
[24] M. D. Kelzenberg, S. W. Boettcher, J. A. Petykiewicz, D. B. Turner-Evans, M. C. Putnam, E. L. Warren, J. M. Spurgeon, R. M. Briggs, N. S. Lewis, H. A. Atwater, *Nat: Mater.* **2010**, *9*, 239.
[25] Efficiency, $\eta = (J_{sc})(V_{oc})(FF)/P$ where P = 100 mW cm^{-2} and *Jsc* is assumed to be 35 mA cm^{-2}. From Table 1 for a polymer-supported wire array at 60 mW cm^{-2} (approximately the same above-bandgap photon flux as 100 mW cm^{-2} AM 1.5), the uncorrected FF = 0.35. Because $V_{oc} = (kT/q)\ln(J_{sc}/J_o)$, increasing J_{sc} from 7.9 to 35 mA cm^{-2} would increase the V_{oc} by 38 mV to V_{oc} = 428 mV. The result is η = 5.2%.